Journal of Materials Chemistry A

Accepted Manuscript

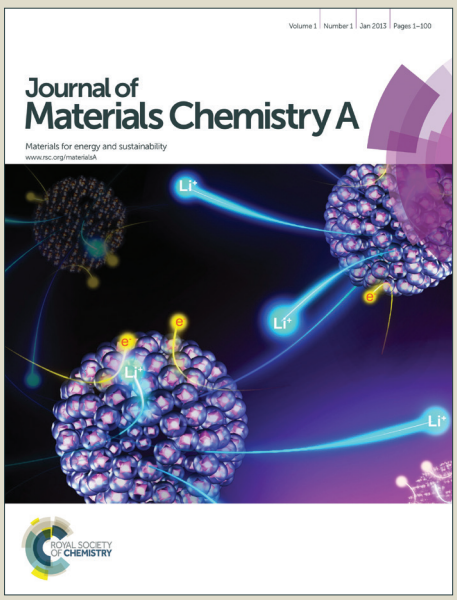

ROYAL SOCIETY OF CHEMISTRY

www.rsc.org/materialsA

3D porous poly (L-lactic acid) foams composed of nanofiber, nanofibrous microsheaf and microsphere, and their application for oil-water separation

Wen Zhang[a], Min Liu[a], Yingying Liu[a], Ruilai Liu[a], Fangfang Wei[a], Rongdong Xiao[b] and Haiqing Liu*[a]

[a]*Fujian Provincial Key Laboratory of Polymer Materials, College of Material Science and Engineering, Fujian Normal University, Fujian 350007, China*

E-mail: haiqing.liu@gmail.com; Fax: +86-591-83404938

[b]*Department of Cardiovascular Surgery, Provincial Clinical College of Fujian Medical University, Fujian 350001, China*

Abstract:

Morphology transition from nanofiber to nanofibrous microsheaf to nanofibrous microsphere was reported for poly(L-lactic acid) (PLLA) induced by thermally induced phase separation of PLLA/dimethylformamide solution. It was found that nanofibrous microsphere, microsheaf, and nanofiber were produced from solutions with PLLA concentration of over 5 wt%, 3 wt%, and 1 wt%, respectively. With respect to the effect of quenching temperature, microsphere and microsheaf were formed at T_q of -10 ^oC and -20 ~ -50 ^oC, respectively. The mechanism of nucleation and crystal growth is responsible for the formation of various PLLA nano-/micro-structures. The foams composed of nanofiber, microsheaf, and microsphere were highly porous in three dimensions with porosity of over 90%. The nano-/micro-dual-scale structure on the foam surface and the trapped air in pores significantly improved the foams' water contact angle to up to 134^o, compared to 79^o of solvent-cast PLLA monolithic film. Due to hydrophobicity, large pore volume and high capillary effect, oil absorption ratio of PLLA porous foams reached up to 1900%. Additionally, such foams absorbed oil in preference to water in an oil-water mixture. In combination with the biodegradable character, those PLLA foams are potential environmental benign oil absorbents and oil-water separation materials.

1. Introduction

Thermally induced phase separation (TIPS) technique is highly efficient in fabrication of three-dimensional (3D) porous structures by a simple procedure, and is easy to control product morphology by adjusting various thermodynamic and kinetic parameters.[1-3] In general, TIPS technique is based on thermodynamic demixing of a homogeneous polymer-solvent system into a polymer-rich phase and a polymer-lean phase by cooling the solution below a spinodal solubility curve.[4, 5]

Ma et al. pioneered the fabrication of PLLA nanofibers through TIPS.[6] They found that the PLLA concentration in tetrahydrofuran (THF) in a range of 1.0 ~ 7.5% (wt/v) had little effect on the morphology of PLLA nanofibers, except some differences in fiber length and pore structure in scaffolds. Yang et al. reported that porous nanofibrous scaffolds were formed from low concentration of PLLA/THF solution, whereas a scaffold similar to a piece of rigid sheet without any pores was obtained from a 9% (wt/v) solution.[7] Solvents employed also affected the morphology of PLLA scaffolds. PLLA scaffolds with regular internal ladder-like, tubular, random and interconnected pore structures were produced when dioxane, benzene and mixed solvent (dioxane/water) were used.[8] With respect to the effect of gelation temperature on morphology and structure of PLLA nanofibers, porous platelet-like and lacy structures were obtained at varied gelation temperature.[9] Therefore, the solution properties and processing parameters play important roles in the morphology of scaffolds.

Until now, THF with low boiling point (T_b = 65 ^oC) is commonly used to prepare PLLA nanofibers by the TIPS method, and randomly organized nanofibrous mats are usually obtained.[10, 11] In this work, *N,N*-dimethylformamide (DMF) is used as a solvent for the first time, not only because it has a T_b of 152.8 ^oC and a freezing point of -61 ^oC, which facilitates the nucleation and crystal growth in the TIPS process, but also two novel and interesting nanostructures, i.e. nanofibrous microsheaf and microsphere, together with nanofibers are developed in the TIPS process.

In the course of TIPS, PLLA/DMF solutions exhibit an upper critical solution temperature (UCST) behavior. Liquid-liquid phase separation and subsequent crystallization is easily achieved by quenching the solution to below its cloud point temperature (T_{cp}). And thus PLLA nanostructures including nanofiber, microsheaf and microsphere from PLLA/DMF solutions are fabricated. The effects of polymer concentration, quenching temperature (T_q) and time on the morphology and crystal structure are studied. Such particular foams composed of nanofiber, microsheaf and microsphere, are highly porous with large amount of capillaries. There are nano-/micro- dual-scale structures on the foam surface and abundant of trapped air in micropores. In view of such special structure and morphology characteristics, the hydrophobicity, oleophilicity, oil absorption and separation of the porous PLLA foams are investigated in detail. The results confirmed that they are promising eco-friendly oil-sorbents and oil-separation materials.

2. Experimental section

2.1. Materials

Poly (L-lactic acid) (PLLA, M_w=100,000) was purchased from Shenzhen Bright Co., China. DMF was bought from Sinopharm Chemical Reagent Co., Ltd. All reagents were analytical grade and used without further purification. Double-distilled deionized water was used.

2.2. Fabrication of PLLA nanostructures by TIPS method

In a typical procedure, 1.0 - 7.0% (weight percent unless specified) homogeneous PLLA/DMF solutions were prepared at 60 ^{o}C for 2 h. Then 8 mL of PLLA/DMF solution was quickly poured into a glass trough (diameter: 7.5 cm). It was immediately quenched at -10, -20, -30 and -50 ^{o}C for a certain time interval. In such a process, different gels were formed (Table 1). Then the gels were immersed into water for solvent exchange. Fresh water was changed three times a day for 2 days. After the gels were removed from water and put into a freezer at -20 ^{o}C for about 5 h, they were freeze-dried at -50 ^{o}C for 48 h. The final dried foams were stored in a desiccator prior to use.

2.3. Characterization

The single point viscosity of PLLA/DMF solutions was measured on a R/S Plus Rheometer (Brookfield) using a C75-1 cone/plate at 25 ^{o}C. A PLLA/DMF solution underwent phase separation when it was cooled down. The T_{cp} was determined by visual inspection of solution clarity upon cooling. Typically, PLLA/DMF solution was pre-heated to 10 ^{o}C above the expected T_{cp} to get a clear solution, which was then slowly cooled in steps of 1 ^{o}C, and maintained for 10 min at each temperature. The

T_{cp} was determined at which the clear solution became turbid.

The surface morphology of PLLA foams was examined on a SEM (JSM-7500F, JEOL) with an accelerating voltage of 3 kV. Samples were platinum-coated before observation. The birefringence of PLLA microsheave and microsphere was observed on a polarized optical microscopy (POM, Leica DMLP). For POM experiment, a dispersion of microsheaf and microsphere in iso-propanol was dropped onto a glass slide and covered with a coverslip. X-ray powder diffraction (XRD) patterns were recorded on a X'pert MPD Pro diffractometer (Philips, Netherlands) with Cu Kα radiation source (λ = 1.542 Å) at a voltage of 40 kV and current of 30 mA. Samples were scanned from 2θ = 5 - 80° at a scanning rate of 8 °/min. The crystallite size was calculated according to Eq. (1):

$$D_{hkl} = \frac{k\lambda}{\beta \cos\theta} \quad (1)$$

where D is the average crystal diameter in Å, λ is the X-ray wavelength (λ = 1.542 Å)，k is the shape factor (k = 0.89), θ is the Bragg angle in degree and β is the line broadening at the half height in radian.

The specific surface area was characterized by a BET method using nitrogen adsorption–desorption isotherm analysis by Belsorp-Max (Japan). The water contact angle (WCA) was carried out by applying 2 μL of liquid droplet onto the PLLA foam surface under ambient laboratory conditions at ~23°C .

The oil absorption capacity was measured by weight measurement. The weighed dry foams were immersed into oils (dodecanol, silicone oil, engine oil (5W-30), and paraffin oil) and were taken out after 5 min at ambient conditions. The oil on the foam

surface was removed with filter papers, then the foam was weighed again. The oil absorption ratio was calculated according to Eq. (2):

$$R_{abs} = \frac{m_a - m_d}{m_d} \times 100\% \quad (2)$$

where R_{abs} is the absorption ratio, m_a and m_d are the mass of the PLLA foams after and before oil absorption, respectively.

In oil-water separation by the PLLA microsphere foam, silicone oil was used as an example oil to investigate the separation of oil from water. The oil-water mixture volume was 100 mL with 1 mL of oil spreading on water surface. The oil layer was dyed with oil blue.

3. Result and discussion

3.1. Morphology of PLLA foams

T_{cp} is the temperature at which an initially homogeneous solution separates into polymer-rich and polymer-lean phases upon thermal treatment. The solution becomes opaque due to refractive index difference of these two phases. From Fig. 1, the T_{cp} almost linearly increases with PLLA concentration. It is -1 and 11^{o}C for PLLA solutions with concentration of 1 and 9%, respectively, suggesting that thermally induced liquid-liquid phase separation temperature of PLLA/DMF solutions increases with PLLA concentration.

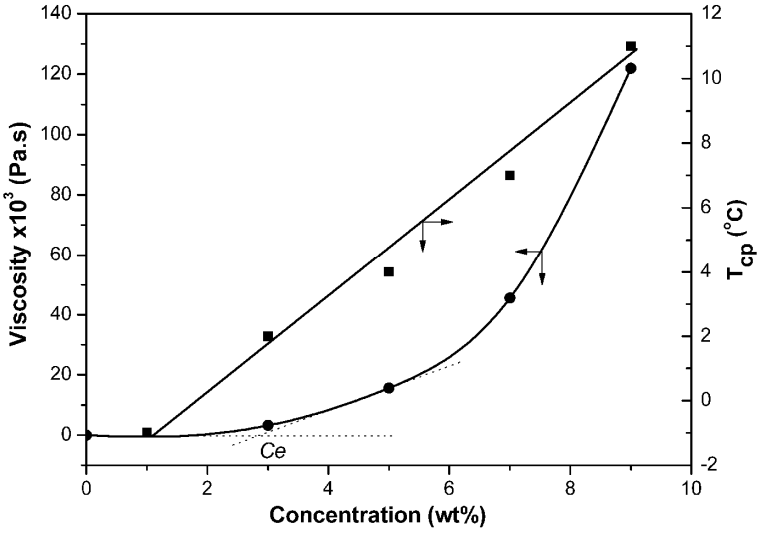

Fig. 1. Relationship of T_{cp} and viscosity with concentration of PLLA/DMF solution.

Upon quenching to below T_{cp}, PLLA/DMF solutions became transparent, translucent or opaque gels depending on T_q and PLLA concentration (Table 1). After solvent exchange and freeze-drying of the gels, PLLA foams with varied nanostructures were generated in quantitative yield (Table 1, Figs. 2 and 3).

Table 1 Summarization of solution state after quenching and the component of PLLA foams

T_q/°C	Solution conc./ wt%	Solution state after quenching	Component of PLLA foam
-10	1	transparent gel	nanofiber
-10	3	translucent gel	nanofiber, microsheaf
-10	7	opaque gel	microsphere
-10	5	transparent gel	microsphere
-20	5	translucent gel	microsheaf and microsphere
-30	5	opaque gel	microsheaf
-50	5	opaque gel	microsheaf

3.1.1. Effect of solution concentration

Fig. 2 shows SEM images of PLLA nanostructures obtained from quenching solutions with various concentrations for different time at -10 °C. For 1% solution, at a short time of 10 min, nanofibers were generated and randomly packed into dense fibrous mats. Similar phenomenon was found with increasing quenching time up to 120 min. The average fiber diameter was 110 - 180 nm, which did not increase with extension of quenching time. Similarly, a PLLA fibrous mat composed of disordered nanofibers was produced at 10 min for 3% solution. As quenching time increased to 50 and 120 min, most nanofibers were apparently bundled together to form sheaf-like structure with obvious stem and branch (Fig. 2h), and the fiber size was 130 - 200 nm. In fact, a few small microsheaves were also observed for the samples of 1%-10, -50, -120 min (Fig. 2a-c) and 3%-10 min (Fig. 2e), as indicated by arrows. In these cases, the stem width of the microsheaf was ca. 0.55 - 0.88 μm, whereas it was increased to ca. 3.70 - 6.90 μm for the samples of 3%-50 and -120 min (Fig. 2f, g). The assembling of PLLA nanofibers altered from microsheaf to microsphere when the PLLA concentration increased from 3% to 5% and to 7%. These highly porous microspheres of ca. 29.00 - 74.10 μm in diameter were composed of fluffy nanofibers with diameter of ca. 150 nm. The porous nanofibrous microspheres formed from 5% solution were not completely isolated from each other, instead they were loosely bridged by a few nanofibers (indicated by arrows). With regard to the fiber length, it varied significantly with PLLA concentration. Fibers were continuous in the longitudinal direction for samples from 1% solution and 3%-10 min (Fig. 2a-e), whereas the microsheaves from 3%-50 and -120 min displayed apparent boundaries

(Fig. 2f, g), indicating their fiber length was limited, similar to the limited size of microspheres from 5% and 7%. The enlarged fine structures of the microsheaves and microspheres are shown in the last column (Fig. 2). Compared to the microspheres from 5% (Fig. 2l), the surface pore size of the microspheres from 7% was larger and more uniform (Fig. 2p). Therefore, the polymer concentration had significant effect on the growth and assembling of PLLA nanofibers.

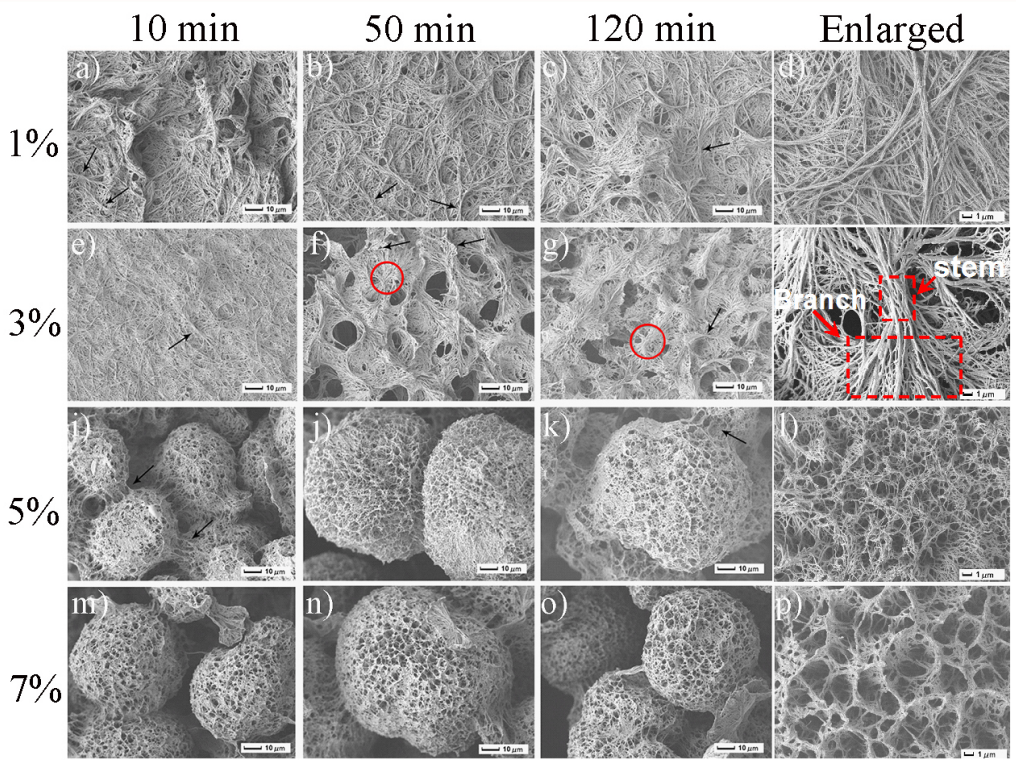

Fig. 2. SEM images of PLLA nanofibers, microsheaves and microspheres as functions of solution concentration and quenching time. Images in the column of 120 min were enlarged in the last column. Solutions were quenched and crystallized at -10 ^{o}C.

As reported by Ma and other researchers, randomly organized PLLA nanofibers were often produced in the TIPS process of PLLA in THF.[12] The mechanism for the formation of nanofibers was related to the liquid-liquid phase separation and

subsequent nucleation and crystallization growth in the polymer-rich phase.[13] By atomic force microscopy, Du et al.[14] observed that PLLA nanofibers grew radially from a nucleus, and a bunch of thin nanofibers further assembled into a big fiber with diameter up to 500 nm. However, PLLA microsheaf and microsphere consisted of nanofibers have not been reported yet before, though these morphologies should be expected if the nucleation and crystallization growth mechanism is able to be applied to the formation of PLLA nanofibers in the TIPS process, just like spherulite crystals are readily produced in the melting process of PLLA.[15] In our study, long PLLA nanofibers were formed from 1% solution and 3%-10 min. Interestingly, large quantities of relatively free spherulites (microsheaf and microsphere) composed of nanofibers were generated from PLLA/DMF solutions with concentration more than 3% (Fig. 2).

The formation of PLLA nanostructures (nanofiber, microsheaf, and microsphere) should be related to the state of PLLA chains in solution. According to the concentration dependence of viscosity of linear polymers in good solvents, there exists four different concentration regimes including dilute, semidilute unentangled, semidilute entangled, and concentrated regimes.[16] The entanglement concentration (C_e) is a boundary between semidilute unentangled and semidilute entangled regimes and defined as the point at which significant overlap of polymer chains topologically constrain chain motion, causing entanglement couplings.[17] On basis of the viscosity ~ concentration relationship shown in Fig. 1, the C_e of PLLA/DMF solution is ca. 2.8%. To large extent, this C_e value was in agreement with the morphology transition as

shown in Fig. 2, i.e. the foams from 1% PLLA solution was almost composed of nanofibers in the quenching time range of 10-120 min, whereas the foams from 3% PLLA solution at quenching time 50 and 120 min were nearly consisted of nanofibrous microsheaf. PLLA chains are relatively free in a semidilute 1% solution. As solution concentration increases to 3%, chains get close and start to entangle. The chain entanglement becomes intense in concentrated solutions (≥5%) (Fig. 3). Upon quenching the 1% solution, chains gradually change their conformation to form crystalline seed nuclei, and growth facets locate at both ends of the nucleus, which guide the crystal growth in one dimension to form linear fibers (Fig. 3). In semidilute entangled 3% solution and at longer quenching time (≥50 min), on the two ends of the nucleus stem, nanofibers grow and split into microsheaves, but their growth ceases when they impinge on another sheaf (Fig. 3), same to the spherulite crystal growth in polymer melts,[18, 19] or fiber network formation in molecular organogel.[20] In concentrated 5 and 7% solutions, chains are intensively entangled and their mobility is constrained, nuclei are readily formed among the closely adjacent pre-ordered chains through orderly packing with the help of hydrophobic interaction. And then chains fold and grow on the crystal growth facets. Due to sufficient amount of PLLA chains around the growing crystals, the crystals grow into spherulites. Similar to the easy formation of spherulites in the crystallization of melt PLLA, high concentration of PLLA chains around the nucleus is a prerequisite for the production of microspheres in the quenched PLLA/DMF solutions (Fig. 2-5% and 7%). Generally the size of microspheres increases with quenching time. For example, in 5% solution,

it increases from ca. 33 to 53 and 67 μm as time extends from 10 to 50 and 120 min. Also it increases from ca. 44 to 72 μm with increasing time from 10 to 50 min in 7% solution (Fig. 2-5% and 7%).

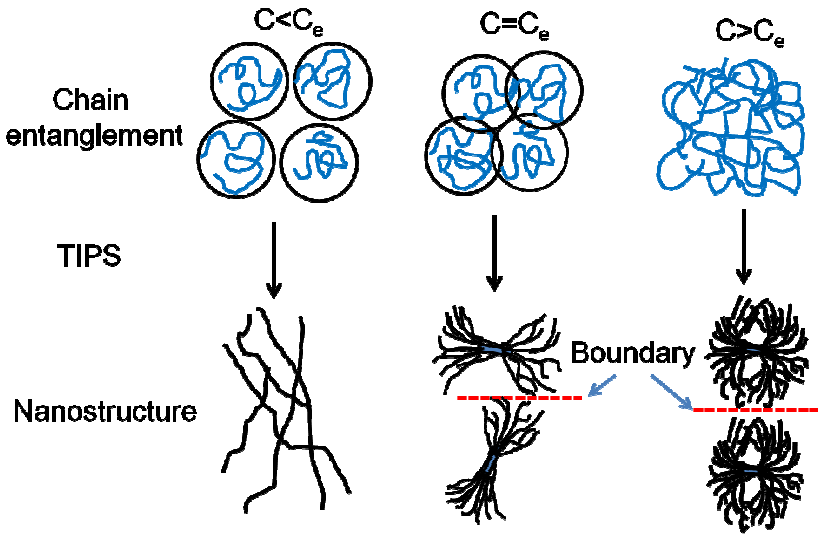

Fig. 3. A cartoon for the formation of nanofiber, microsheaf, and microsphere from PLLA/DMF solutions with varied concentrations by TIPS. C_e is ca. 2.8% for this solution.

3.1.2. Effect of T_q

The effect of T_q and quenching time on the morphology of PLLA nanostructures is shown in Fig. 4. At -10 ^oC, microspheres with lacy surface structure and average diameter of about 44.2 - 60.3 μm were generated in the time range of 10 - 90 min. At -20 ^oC, large amount of distinct nanofiber microsheaves were observed when quenched for 10 min, while extensively intertwisted nanofiber sheaves (Fig. 4h) were produced at 50 min, microspheres were formed at 90 min. When crystallized at lower temperatures of -30 and -50 ^oC, only nanofiber microsheaves were got. At corresponding time, the average size of microsheaves at -30 ^oC was generally bigger

than that at -50 °C. In order to reduce surface stress,[21] long nanofiber microsheaves would tilt and distort, and even intertwine together (Fig. 4h, l, p).

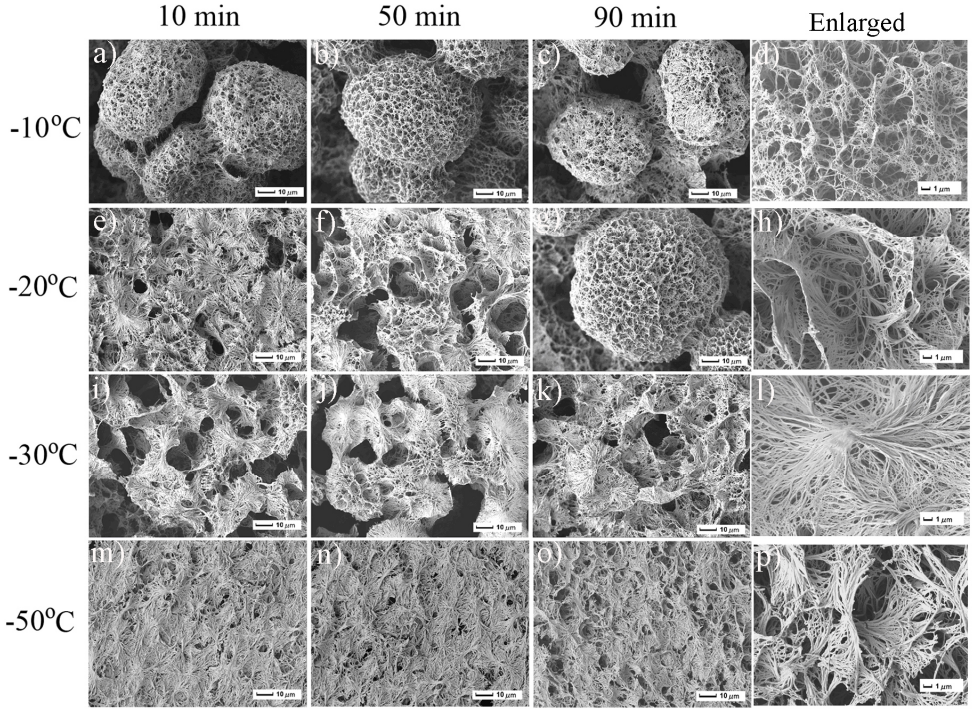

Fig. 4. SEM images of PLLA microspheres and microsheaves as functions of quenching time and temperature. Images in the 50 min column were enlarged in the last column. PLLA solution concentration was 5%.

The SEM images further demonstrated that PLLA foams were composed of microspheres (Fig. 5a) and microsheaves (Fig. 5e) in the cross-sectional direction, proving that the physical structure was uniform from top to inside of the foams. The microsphere was nearly a perfect spherical shape (Fig. 5c), and it was consisted of nanofibers (Fig. 5d). Large amount of pores/capillaries were present among those nanofibers.

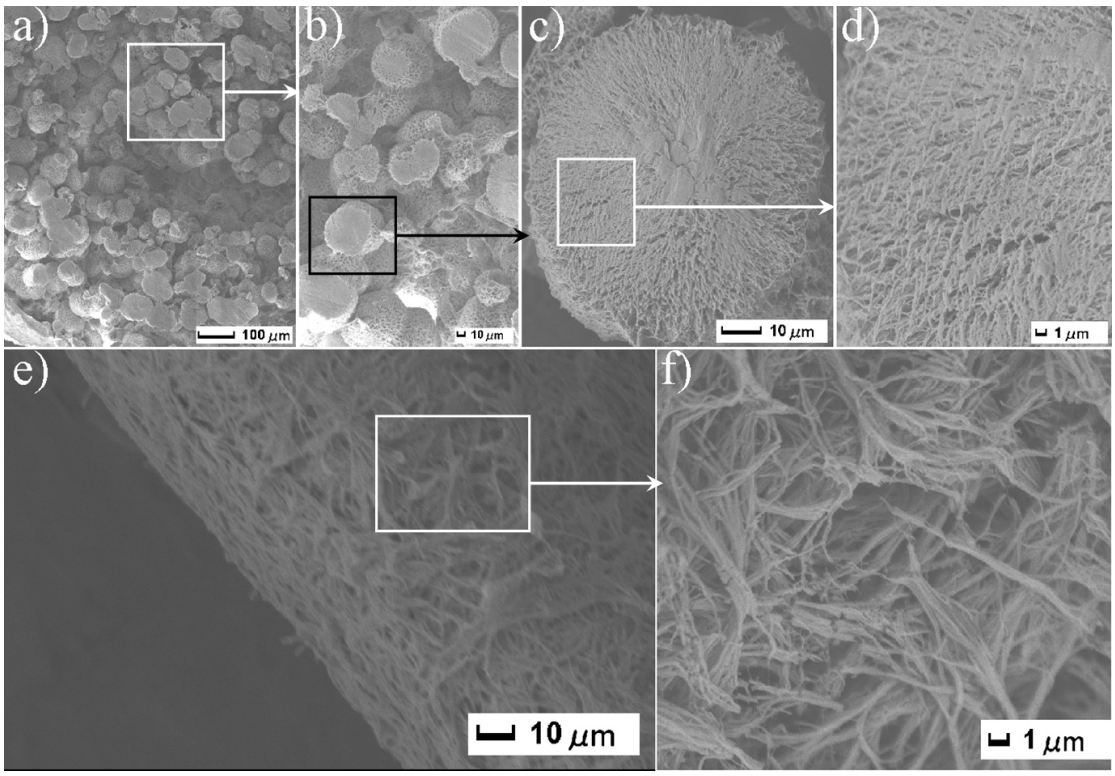

Fig. 5. Cross-sectional SEM images of PLLA foams composed of (a) microspheres (sample shown in Fig. 4b), and (e) microsheaves (sample shown in Fig. 4n).

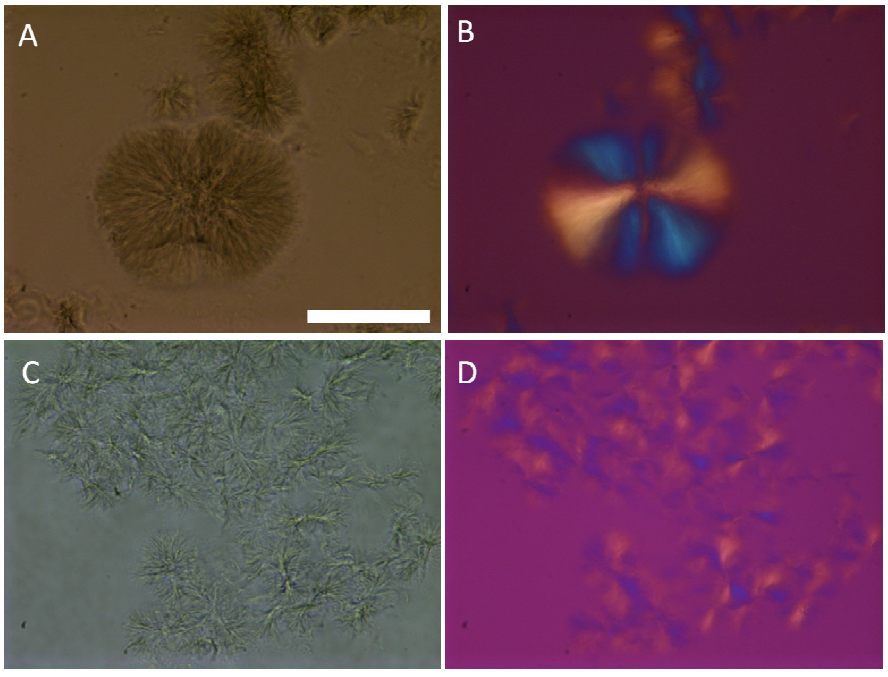

Fig. 6. Optical microscopy images of (A) microspheres (shown in Fig. 4b) and (C) microsheaves (shown in Fig. 4n), and (B, D) corresponding polarized microscopy. Scale bar is 50 μm, and applied to all images.

The POM images of PLLA microspheres and microsheaves displayed Maltase-cross pattern (Fig. 6B, D), which was a characteristic proof that these microstructures were spherulite crystals. Therefore, it is out of question that nucleation and crystal growth mechanism are involved in the formation of microspheres and microsheaves in the PLLA-rich phase upon TIPS. And thus the T_q would play a crucial role in controlling the morphology of PLLA nanostructures by affecting chain mobility, nucleation and growth kinetics in solutions. Specifically, the PLLA nanostructures in the TIPS process is related to quenching depth, which is defined as the temperature difference between T_{cp} and T_q, i.e. $\Delta T = \left| T_q - T_{cp} \right|$. The T_{cp} of 5% PLLA/DMF solution is 4 ^{o}C (Fig. 1). When it is quenched to -10, -20, -30, and -50 ^{o}C, the quenching depth is 14, 24, 34 and 54 ^{o}C, respectively. Deeper quenching depth leads to stronger driving force for the formation of nucleus.[22] However, the chain segment would be less mobile at lower temperatures. At -10 ^{o}C, the formation of PLLA nucleus is slow, and it has a relatively low PLLA nucleus density in the gel, but the freedom of chain segment movement and rotation is relatively high, so the crystals grow up into microspheres. At -20 ~ -50 ^{o}C, on one hand, the chain mobility is low; on the other hand, the nucleation rate is fast and nucleus density is high, resulting in fewer chains available to each nucleus. This leads to the formation of many nanofiber microsheaves instead of microspheres (as shown for samples at -20 ^{o}C), and to the formation of smaller sheaves at -50 ^{o}C than at -30 ^{o}C at corresponding quenching time of 50 min and 90 min (Fig. 4). In the crystallization of molten PLLA,

it has been found that when crystallization is performed at high undercooling, the reduced molecular mobility enhances the nucleation rate as compared to the crystal growth rate, leading to the formation of a high number of smaller crystals.[23]

3.2. XRD patterns of PLLA nanostructures

Fig. 7 shows XRD patterns of the PLLA foams prepared from quenching at -10, -30 and -50 ^{o}C for 50 min. All samples displayed two diffraction peaks for (110)/(200) and (203) planes, which located at ca. 2θ = 16.4° and 18.8°. The crystalline structure was assigned to α' phase PLLA.[14] As shown in Table 2, the crystallite size slightly decreased from 12.5 to 11.9 nm with T_q reducing from -10 to -50 ^{o}C. These results suggested that PLLA in DMF solution formed α'-crystal at $-10 \leq T_q \leq -50$ ^{o}C. According to Zhang et al.,[24] the structural difference between α'- and α-crystal was related to the chain conformation and packing mode, the α'-crystal possessed a relatively looser and disordered structure than α-crystal. It is also known that α'-form PLLA is less unstable, and can be transformed to α-form in some conditions. Pan et al.[25] reported that α'-form PLLA was changed to α-form upon annealing at elevated temperatures. Similar phenomenon was also observed by Cocca et al.[26] In our experiment, a typical sample (obtained from quenching 5% solution at -30 ^{o}C for 50 min) was annealed at 115 ^{o}C for 5 h. Its XRD pattern presented two more diffraction peaks at 15.14^{o} and 26.05^{o} for respective (010) and (206) crystal planes, which were characteristic peaks of α-form PLLA crystal. The peak intensity at 16.4° and 18.8° also increased significantly. The crystallite size increased greatly from 12.5 to 23.0 nm after

annealing.

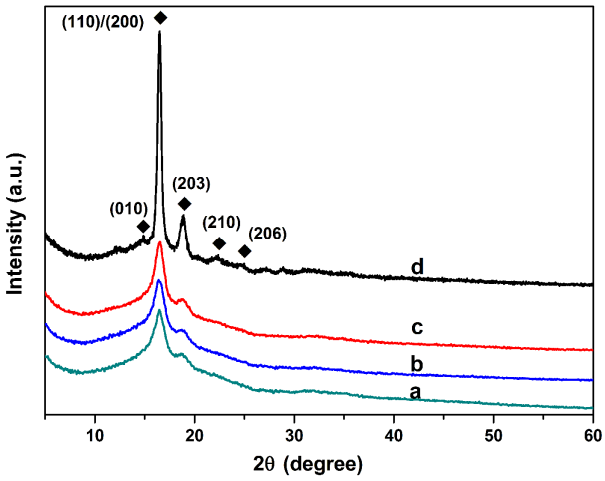

Fig. 7. XRD patterns of PLLA foams obtained from 5% PLLA/DMF solution quenched for 50 min at (a) -10 °C; (b) -30 °C; (c) -50 °C; (d) sample b was annealed at 115 °C for 5 h.

Table 2 XRD results of PLLA foams obtained from 5% PLLA/DMF solution quenched at different temperature for 50 min

Entry	T_q/°C	2θ at crystal plane/degree					crystallite size
		010	110/200	203	210	206	(nm)
1	-10	-	16.54	18.98	-	-	12.50
2	-30	-	16.38	18.70	-	-	12.50
3	-50	-	16.43	18.81	-	-	11.90
4[a]	-30	14.85	16.48	18.89	22.37	24.97	23.00

[a]Entry 4 was obtained by annealing entry 2 at 115 °C for 5 h.

3.3 Oil absorption and separation

The contact angle of a material is highly dependent on its surface topography. A surface with nano-/micro- dual-scale morphologies and entrapped air would give it high hydrophobicity.[27, 28] Superhydrophobic porous materials have been extensively

studied for application in the field of oil absorption and separation.[29, 30] Due to the nano-/micro- morphologically rough surfaces of the PLLA foams composed of nanofiber, nanofibrous microsheaf and nanofibrous microsphere, the WCA was significantly raised to 105.4±1.1°, 118.5±0.8°, and 134.2±1.4° for the nanofiber, microsheaf and microsphere foams, respectively (Fig. 8), as compared to 79.5±0.3° for the solvent-cast monolithic PLLA film (Fig. 8a). Therefore, the hydrophobicity of these special PLLA foams was improved greatly; Additionally, the hydrophobicity increased with the surface roughness as displayed in the SEM images of nanofiber foam (Fig. 2b), microsheaf foam (Fig. 4n) and microsphere foam (Fig. 4b). In a typical example, silicone oil was absorbed by the microsphere foam in ca. 3 seconds (Fig. 8d), displaying apparent contact angle of 0°. Quick oil absorption was also observed on nanofiber and microsheaf foams. This observation suggests that these foams are highly oleophilic materials.

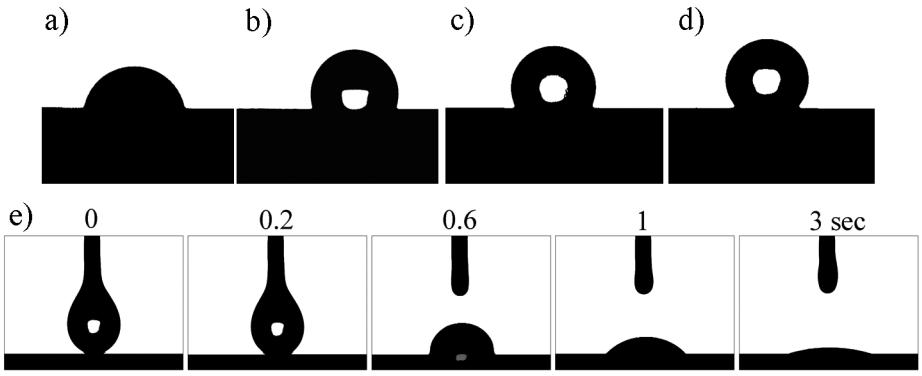

Fig. 8. A water droplet on (a) solvent-cast PLLA film (WCA=79.5±0.3°), (b) PLLA nanofiber foam (WCA=105.4±1.1°), (c) PLLA microsheaf foam (WCA=118.5±0.8°), (d) PLLA microsphere foam (WCA=134.2±1.4°). (e) Evolution of a silicone oil droplet on a PLLA microsphere foam. The microsheaf foam and microsphere foams are samples shown in Fig. 4n and 4b, respectively.

Table 3 WCA, porosity and density of some typical samples

Sample	Source	Density (g/cm^{-3})	BET surface area(m^2/g)	WCA (^{o})	Porosity (%)
Solvent-cast film	--	1.31	0.63	79.5±0.3	Not measured
Nanofiber foam	Fig. 2b	0.115	13.8	105.4±1.1	89.3
Microsheaf foam	Fig. 4n	0.083	14.2	118.5±0.8	93.4
Microsphere foam	Fig. 4b	0.072	16.1	134.2±1.4	94.6

Some important physical properties of the PLLA foams are listed in Table 3. The density of PLLA nanofiber, microsheaf and microsphere foams is 0.072-0.115 g/cm^3, which is just 5.5-8.8% of that of the solvent-cast PLLA film. The BET surface area of the foams is 20-25 times larger than that of the film, and increases in an order of nanofiber foam < microsheaf foam < microsphere foam. The nanofibers packed together more closely than microsheaves and microspheres (Fig. 2b, 4b, 4n), leading to a higher density but smaller porosity. Because of high hydrophobicity and oleophilicity and large porosity, the PLLA foams display high oil absorption efficiency. Among the three foams, the nanofiber foam shows the least oil absorption ratio, which is ca. 800-1200%, while the microsphere foam has the highest oil absorption ratio, i.e. 1500-1900%. This value is about 20 times larger than the counterpart PLLA film (Fig. 9). Judging from the density of the oils (it is 0.862, 0.963, 0.877, and 0.835 g/cm^{-3} of engine oil, silicone oil, paraffin oil and dodecanol oil, respectively), it is thought that the porosity difference among the foams is accountable for the oil absorption variation since the absorption mechanism is

merely a physical storage of oil in the foam pores. The oil absorption capacity highly depends on the pore structure of oil sorbents. In our previous work, we found that electrospun PLLA nanofibrous mats (with meso-/micro- pores on and within fibers) could absorb 90 g/g pump oil.[31] Ding et al. reported that the electrospun polystyrene fibrous mats (with large amount of pores in the internal fiber) absorbed ca. 80 g/g motor oil.[32] Though the oil absorption capacity of the PLLA foams from TIPS was less than that of the electrospun PLLA nanofibrous mat, the former with absorbed oil kept their shape well, while the latter tended to disintegrate to some extent. The good shape maintainability helps easily recycle when needed.

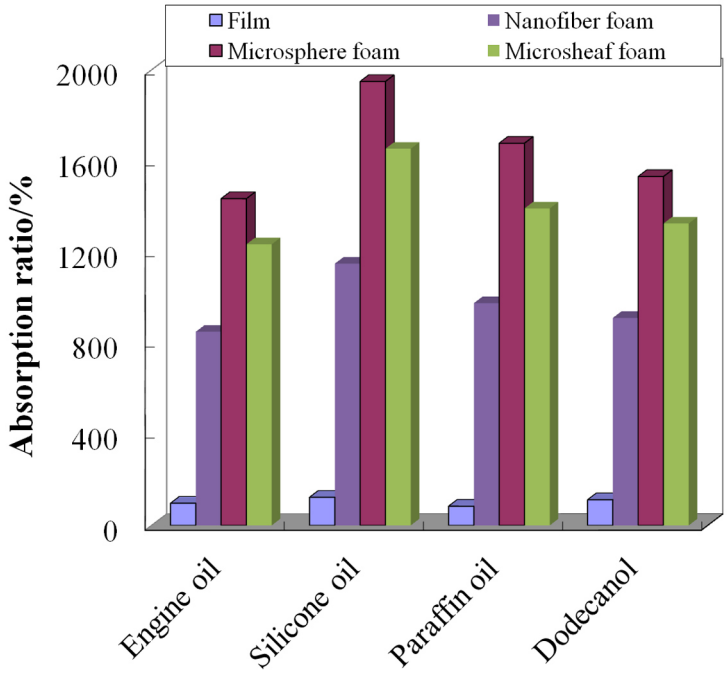

Fig. 9. Oil absorption ratio of PLLA film, nanofiber foam (sample of Fig. 2b), microsphere foam (sample of Fig. 4b), and microsheaf foam (sample of Fig. 4n).

The hydrophobicity in combination with oleophilicity make the PLLA foam not only a good oil absorbent, but an efficient oil-water separation material. In a typical example, when a dried PLLA microsphere foam (thickness: 2.3 mm) was brought into

contact with an oil layer drifting on water (Fig. 10 a), the foam quickly (within 2-3 seconds) absorbed the blue oil layer while repelling water. The oil absorbed microsphere foam was easily recovered since it still drifted on water (Fig. 10b). Clear water was left behind after the foam was taken out (Fig. 10c). No size and shape change was observed for the oil absorbed foam, suggesting that oil was physically held in foam's pores and capillaries. The other two PLLA foams also showed efficiently preferred oil absorption over water, making the PLLA foams promising candidates for oil-water separation. They may be applied to clean up oil contaminated water. Compared to the well-studied oil sorbents like electrospun polystyrene fibers,[32, 33] carbon nanofibers,[34] and commercialized polypropylene non-woven mat, the readily biodegradability of PLLA makes PLLA foams environmental benign oil-sorbent and oil-water separation materials.

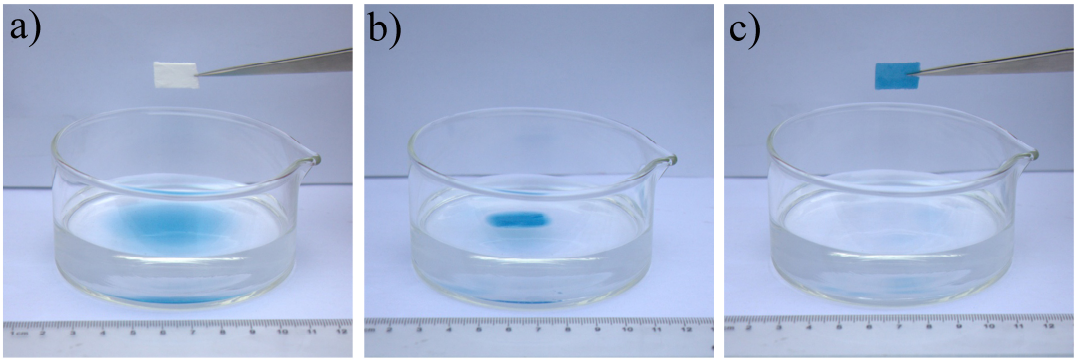

Fig. 10 Separation of silicone oil layer spreading on water surface by the PLLA microsphere foam. The oil layer was doped with oil blue. (a) before, (b) during, and (c) after oil/water separation.

4. Conclusion

PLLA foams composed of nanofiber, nanofibrous microsheaf and microsphere were prepared from its DMF solutions by the TIPS method. Such nano-/micro-structures were functions of solution concentration, quenching temperature, and quenching time. When PLLA/DMF solutions were quenched at -10 ^{o}C for 10 - 120 min, continuous nanofibers were formed from the 1% PLLA/DMF solution; microsheaves were the main morphology from 3% solution; and microspheres were generated from 5 - 7% solutions. Low quenching temperature at -10 ^{o}C for 5% PLLA/DMF solution led to the formation of microspheres, whereas lower quenching temperature at -20 ~ -50 ^{o}C gave microsheaves. The formation of varied PLLA nanostructures was induced by the liquid-liquid phase separation but controlled by the nucleation and crystal growth mechanism. PLLA microsheaf and microsphere showed characteristic Maltase-cross pattern, proving that they belonged to spherulite crystals. Loosely chain packing and less ordered α'-form PLLA was formed in these nanostructures. The rough surface with nano-/micro- dual-scale topography and trapped air in micropores greatly improved the PLLA foams' water contact angle to 105 - 134^{o}, making them highly hydrophobic. In combination with oleophilicity and large porosity, the PLLA foams could absorb oil of as much as 19 times more than its dry weight; additionally, they were capable of efficiently and quickly separate oil from water in an oil-water mixture. The PLLA foams prepared in this study are promising environmentally friendly oil absorbents and oil/water separation materials.

Acknowledgements

This work is supported by the Research Fund for the Doctoral Program of Higher Education of China (No. 20123503110003), Natural Science Foundation of Fujian Province (2010J06017), Education Department of Fujian Province (JA13079), Key Project of Science and Technology Department of Fujian Province (2013Y0027).

Notes and references

1. Y. S. Nam and T. G. Park, *J. Biomed. Mater. Res.*, 1999, **47**, 8-17.
2. T. Qu and X. Liu, *J. Mater. Chem. B*, 2013, **1**, 4764-4772.
3. J. M. Holzwarth and P. X. Ma, *J. Mater. Chem.*, 2011, **21**, 10243-10251.
4. R. Bansil and G. Liao, *Trends Polym. Sci.*, 1997, **5**, 146-154.
5. G. Jell, R. Verdejo, L. Safinia, M. S. P. Shaffer, M. M. Stevens and A. Bismarck, *J. Mater. Chem.*, 2008, **18**, 1865-1872.
6. P. X. Ma and R. Y. Zhang, *J. Biomed. Mater. Res.*, 1999, **46**, 60-72.
7. F. Yang, R. Murugan, S. Ramakrishna, X. Wang, Y. X. Ma and S. Wang, *Biomaterials*, 2004, **25**, 1891-1900.
8. G. Wei and P. X. Ma, *Biomaterials*, 2004, **25**, 4749-4757.
9. He L M, Zhang Y Q and Z. X, *Polymer*, 2009, **50**, 4128-4138.
10. X. Wang, G. Song and T. Lou, *J. Mater. Sci. -Mater. Med.*, 2010, **21**, 183-188.
11. H. Ma, J. Hu and P. X. Ma, *Adv. Funct. Mater.*, 2010, **20**, 2833-2841.
12. H. Y. Ma, J. A. Hu and P. X. Ma, *Adv. Funct. Mater.*, 2010, **20**, 2833-2841.
13. R. Liu, K. Li, M. Liu, Y. Liu and H. Liu, *J. Polym. Sci. B Polym. Phys.*, 2014, **52**, 1476-1489.
14. J. Shao, C. Chen, Y. Wang, X. Chen and C. Du, *Appl. Surf. Sci.* , 2012, **258**, 6665-6671.
15. W. C. Lai, *Soft Matter*, 2011, **7**, 3844-3851.
16. R. H. Colby, L. J. Fetters, W. G. Funk and W. W. Graessley, *Macromolecules*, 1991, **24**, 3873-3882.
17. W. W. Graessley, *Polymer*, 1980, **21**, 258-262.
18. L. Bouapao, H. Tsuji, K. Tashiro, J. Zhang and M. Hanesaka, *Polymer*, 2009, **50**, 4007-4017.
19. B. C. Okerberg, B. C. Berry, T. R. Garvey, J. F. Douglas, A. Karim and C. L. Soles, *Soft Matter*, 2009, **5**, 562-567.
20. R. Y. Wang, X. Y. Liu, J. Xiong and J. Li, *J. Phys. Chem. B*, 2006, **110**, 7275-7280.
21. B. Lotz and S. Z. Cheng, *Polymer*, 2005, **46**, 577-610.
22. M. Salmerón Sánchez, V. B. Mathot, G. Vanden Poel and J. L. Gómez Ribelles,

Macromolecules, 2007, **40**, 7989-7997.
23. S. Iannace and L. Nicolais, *J. Appl. Polym. Sci.* , 1997, **64**, 911-919.
24. Y. Zhang, J. Venugopal, Z. M. Huang, C. Lim and S. Ramakrishna, *Biomacromolecules*, 2005, **6**, 2583-2589.
25. P. Pan, B. Zhu, W. Kai, T. Dong and Y. Inoue, *Macromolecules*, 2008, **41**, 4296-4304.
26. M. L. Di Lorenzo, M. Cocca and M. Malinconico, *Thermochim. Acta* 2011, **522**, 110-117.
27. P. Roach, N. J. Shirtcliffe and M. I. Newton, *Soft Matter*, 2008, **4**, 224-240.
28. T. L. Sun, L. Feng, X. F. Gao and L. Jiang, *Acc. Chem. Res.*, 2005, **38**, 644-652.
29. Q. Zhu, Y. Chu, Z. Wang, N. Chen, L. Lin, F. Liu and Q. Pan, *J. Mater. Chem. A*, 2013, **1**, 5386-5393.
30. Y. Shang, Y. Si, A. Raza, L. Yang, X. Mao, B. Ding and J. Yu, *Nanoscale*, 2012, **4**, 7847-7854.
31. S. Cao, B. Hu and H. Liu, *Acta Polym. Sin.*, 2010, **10**, 1193-1198.
32. J. Lin, B. Ding, J. Yang, J. Yu and G. Sun, *Nanoscale*, 2012, **4**, 176-182.
33. M. W. Lee, S. An, S. S. Latthe, C. Lee, S. Hong and S. S. Yoon, *ACS Appl. Mater. Interface*, 2013, **5**, 10597-10604.
34. H. Liu, C.-Y. Cao, F.-F. Wei, P.-P. Huang, Y.-B. Sun, L. Jiang and W.-G. Song, *J. Mater. Chem. A*, 2014, **2**, 3557-3562.

TOC

3D porous poly (L-lactic acid) foams composed of nanofibers, nanofibrous microsheaves and microspheres, and their application for oil-water separation

Wen Zhang, Min Liu, Yingying Liu, Ruilai Liu, Fangfang Wei, Rongdong Xiao, and Haiqing Liu

Highly hydrophobic PLLA foams composed of nanofibrous microsheaf and microsphere were fabricated and applied as an oil-water separation material.